Journal of Low Temperature Physics, Vol. 46, Nos. 5/6, 1982

Photographic Studies of Quantized Vortex Lines*

E. J. Yarmchuk† and R. E. Packard

Physics Department, University of California, Berkeley, California

(Received August 26, 1981)

A study of the behavior of systems of quantized vortex lines in rotating superfluid ^4He is described. Using a photographic technique, the positions of the vortex cores at the free surface of the liquid are recorded in the form of time-lapse motion pictures. The observation of stationary arrays of vortices are discussed and a comparison with the predictions of rectilinear vortex theory is made. Discrepancies between the observations and this theoretical model are noted, and the limitations of the experimental method are described. Several distinct types of periodic array motion have been observed. A description of their analysis as well as possible theoretical and experimental interpretations are given. The final part of this study involves phenomena associated with acceleration of the vessel. The analysis of film records and light signal amplitude measurements for repeated spinups of the vessel reveals statistical trends in the rate of appearance of vortices.

1. INTRODUCTION

The technique of photographing the positions of quantized vortex lines in superfluid helium is potentially capable of permitting detailed studies of vortex dynamics. In several previous papers from this laboratory[1,2] we have described the experimental method and given a short description of observations of stationary vortex states. This paper is intended to be a more complete description of observations made using this technique.

Very briefly, the photographs are produced in the following manner. Ions (electron bubbles) are injected into a rotating vessel of superfluid ^4He, where they are attracted toward and become trapped on the cores of the vortices. After a sufficient amount of charge has accumulated (this takes about 10 s) an electric field is applied which pulls the ions along the cores and through the surface of the liquid at the top of the vessel. The ions, which become free electrons as they emerge from the liquid, are accelerated

*This work was supported by the National Science Foundation (Grant No. DMR 76-82934).
†Present address: IBM Thomas J. Watson Research Center, Yorktown Heights, New York.

0022-2291/82/0300-0479$03.00/0

and focused onto a phosphor screen. The fluorescent pattern produced by the phosphor maps the positions of the vortices where they intersect the surface of the liquid. The light signals produced in the low-temperature cell are transmitted to room temperature via coherent fiber optics. The images (produced at regular intervals, typically 10–20 s) are captured by a single-frame, low-light-level television system and recorded on successive frames of motion picture film. A block diagram of the apparatus is shown in Fig. 1, and the essential features are described in the legend. A more complete description of the apparatus is given in Ref. 1.

Basically, data are obtained by rotating the apparatus and recording on film the positions of the vortices which appear. A particular procedure which has been quite useful is the filming of sequences of spinup trials. Each trial consists of a uniform angular acceleration (~ 0.02 rad/sec^2) from rest to some rotation speed. This speed is maintained for a predetermined length of time (typically 1 h), after which the apparatus is brought to rest by uniform angular deceleration. A digitally derived voltage ramp applied to the drive motor of the apparatus is used to control the rate of angular acceleration. Sequences of trials were obtained by repeating these spinups at regular intervals (usually 1 h at rest between trials). In a given sequence, all trials have the same rotation speed and acceleration. This procedure allows the reproducibility of observed phenomena to be studied.

Another procedure is one in which the apparatus is brought from rest to a fixed rotation speed by manually increasing the voltage applied to the drive motor. In these cases, constant-rotation-speed filming continues for times as long as 25 h. A third procedure involves very slow accelerations ($\sim 10^{-5}$ rad/sec^2). Beginning at rest, the uniform angular acceleration proceeds until an angular velocity of approximately 0.9 rad/sec is reached, at which point the speed is held constant. Since the rate of angular acceleration is determined by the frequency of pulses which are counted and applied to a digital-to-analog converter (which produces the waveform applied to the drive motor), a constant acceleration can be maintained over the long periods of time which are required (~ 25 h). The duration of any trial is limited to approximately 30 h because of the loss of liquid helium from the reservoir of the refrigerator. Sequences of trials can be continued for much longer periods by replenishing the reservoir during one of the rest periods preceding each spinup.

Three types of analysis are used to extract information from the motion picture film records. The first is simply to view the projected films at speeds of 6 or 18 frames per second. Since the real time interval between frames is 10 s or more, the projected film greatly compresses the time span of the observations and allows a rapid determination of the general sequence of observed events. An initial evaluation of all films was made in this way.

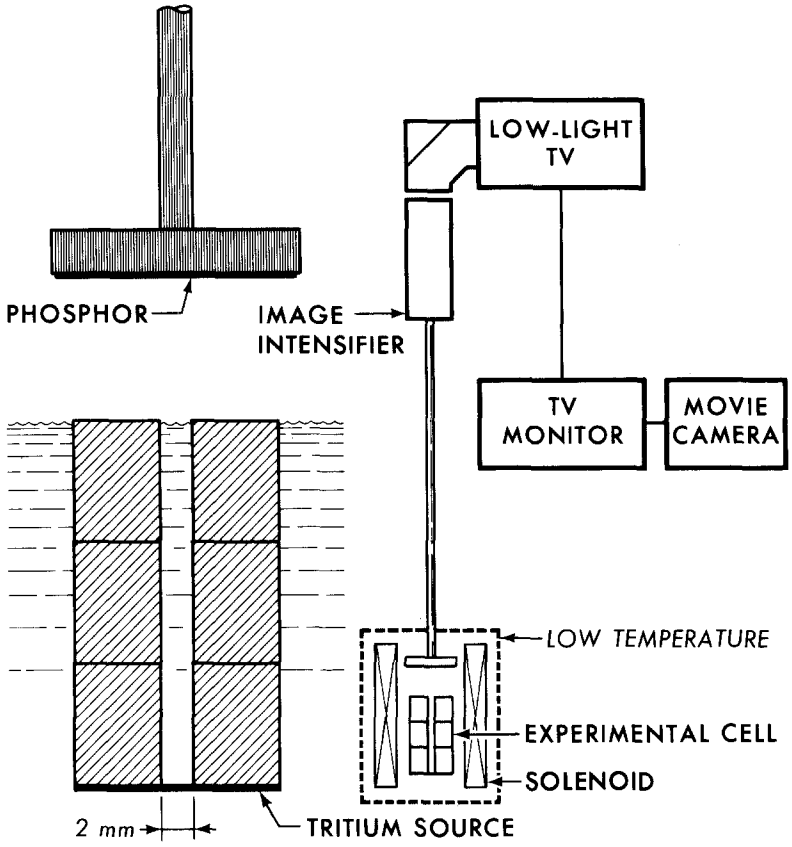

Fig. 1. A block diagram of the apparatus. The cylindrical vessel is a 2-mm-diameter hole drilled in a stack of three carbon composition resistors. It is 22.7 mm in height. Voltage differences applied across each resistor section produce axial electric fields for the manipulation of the ions. A tritiated titanium foil forms the bottom surface of the vessel and serves as the ion source. A 700-V potential difference is applied between the phosphor screen and the top of the vessel for acceleration of the electrons. The solenoid produces a magnetic field of 0.5 T, which prevents defocusing of the accelerated electrons.

For the second type of analysis multiple exposure prints of sequences of film frames are produced by projecting a portion of the film onto a piece of photographic paper. In this way, many of the films have been reduced to a series of prints, each of which is a multiple exposure of approximately 60 film frames. The motion picture projector produces a reasonably accurate reproduction of the film images, but care must be taken if quantitative information is to be extracted from such prints. Nevertheless, the multiple

exposure prints are quite useful in the display of qualitative aspects of the observations. A third technique has been used for the extraction of quantitative data (such as the separation of vortex images). Here we have made use of the technology developed for the accurate analysis of bubble chamber photographs. Using a film scanning machine, one can determine the positions of the vortex images from the film itself and, with a calibration determined from a test pattern (discussed below), quantitative results can be obtained. Because it is so time-consuming, only ~1% of the 300,000 film frames have been analyzed in this way.

The calibration of the optical system is not entirely straightforward and requires some discussion. The imaging system can be divided into three parts, the electron optical system within the cell, the fiber optics image conduit, and the remaining, room-temperature components. The room-temperature components (the image intensifier, the television camera, the television monitor, and the movie camera) are maintained in a fixed configuration and can be calibrated as a group by means of a test pattern. We use an electroformed pinhole grid which has a triangular lattice of holes [measured to be $(5.58 \pm 0.02) \times 10^{-2}$ cm on a side]. The pattern is inserted at the butt joint between the room-temperature end of the cryostat image conduit and the input of the image intensifier (a fiber optics faceplate). Very little illumination is required and is provided by light scattered into the unshielded image conduit when a light bulb in the dewar is turned on. The pattern is recorded on film in the same manner as the vortex film sequences. Measurement of the recorded pattern with the film scanner yields the overall image magnification (for this part of the system) with an accuracy of about 2%. Most of the uncertainty arises from optical distortion, which causes roughly 2% variations in scale over the region of interest. The fiber optics image conduit is expected to produce a magnification of very nearly unity. At room temperature the magnification is measured to be 1.0015 ± 0.0038. During the experimental run, however, contraction of the cold end relative to the warm end would produce an image size increase of approximately 1%.

While it would be desirable to have had an in situ calibration of the low-temperature electron optics part of the imaging system, the practical complications involved with such a scheme are great. It is possible, however, to estimate the effects of electrode geometry and magnetic field configuration. The electrode geometry in the acceleration region is approximately that of parallel plates, one at the phosphor screen and the other at the liquid surface. The metal plates are 1.9 cm in diameter and are separated by 1 cm. The phosphor itself is 5 mm in diameter and located within a 6-mm-diameter hole at the center of the upper plate. Underlying the phosphor is a transparent conductive coating of tin oxide. The top of the

2-mm-diameter vessel forms a circular aperture in the lower plate. The emerging low-energy electrons are most strongly affected by field inhomogeneities in the region of this aperture. Numerical calculation of the electron trajectories for a model in which the accelerating electric field is that due to a circular aperture in an infinite conducting plane[3] show that the deviations of the paths away from the magnetic field lines are negligibly small except for electrons that originate extremely close to the edge of the aperture (which corresponds to the vessel wall in this model). Electric field inhomogeneities matter very little because the focusing magnetic field (see Fig. 1) is so large (0.5 T). Thus it seems that the details of the electrode configuration can be justifiably ignored and the problem reduced to that of the magnetic field alone. Calculation of the spreading of the magnetic field lines due to the finite length of the solenoid (15 cm long, 10 cm in diameter) yields an expected image magnification of 1.016 ± 0.002. (The 1-cm drift region is approximately 5 cm inside the end of the solenoid.)

The basic photographic method has several aspects which have to be considered in interpreting the data. Of prime importance is the fact that the pictures only show the positions of the vortices at the free surface of the liquid. Since it is very possible that the lower end of the vortex lines may be tightly pinned to the vessel's side or bottom, we cannot assume that the lines are simple rectilinear structures. Indeed, in what follows, pinning seems the most likely mechanism to explain differences between two-dimensional theory and the data.

A less fundamental weakness in our particular apparatus lies in the image conduit which transmits the image to room temperature. Examination of the fiber optics shows isolated regions of poor transmission, presumably because of broken fibers. Furthermore, we have observed that fiber optics butt joints in our system produce a Moiré pattern of transmitted light. Figure 2 shows the uneven transmission of this element. Although we lack conclusive proof, there is evidence (discussed in the next section) which indicates that images are occasionally "missing" as a result of some mechanism other than the actual disappearance of a vortex. The imperfections in the image conduit could produce such an effect.

A final point is that bright noise flashes within the image intensifier (arising from the ionization of gas atoms) produce images similar to those of vortices. Under optimum conditions, the probability that a given film frame contains a "false" image within an area the size of the vessel opening is measured to be approximately 3%. While only the brightest of the noise flashes are comparable in intensity with the vortex signals, saturation of the television signal can cause weaker flashes to appear relatively intense if the gain is too high. Some of the films possess unnecessarily high noise levels because gain drifts (associated with temperature changes of the room)

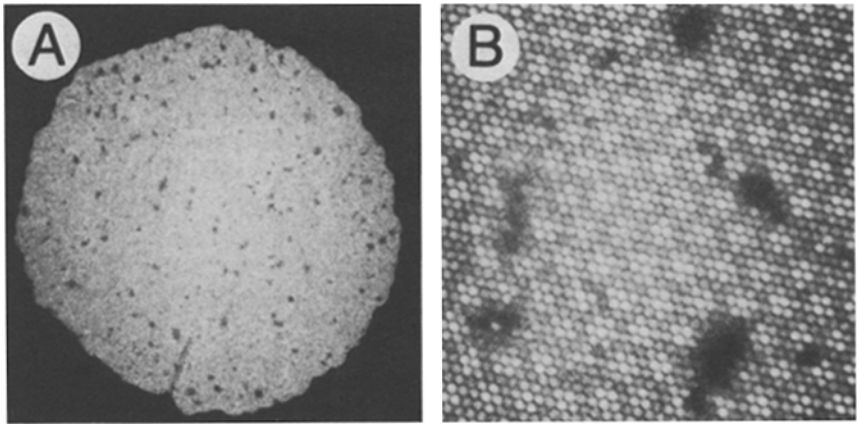

Fig. 2. Transmitted light photographs of the fiber optics image conduit. Photograph A shows the entire field of the 3.2-mm-diameter image conduit, while B is an enlargement of a small area and clearly shows the individual fibers (11.6 μm diameter). The Moiré pattern produced by the butt joint between the two sections of image conduit can also be seen in B.

caused such saturation. Noise suppression by means of multiply exposed prints is quite useful in such cases.

The remainder of this paper is divided into three sections. In the next section we concentrate on observations of stationary states. Then Section 3 discusses data showing periodic vortex motion. The final section presents results of "spinup" experiments which shed light on the topic of how vortices enter the rotating helium.

2. STATIONARY ARRAYS

The nature of the equilibrium state of superfluid helium in a rotating vessel has been investigated theoretically by a number of authors.[4,5] The most extensive analysis is that of Campbell and Ziff,[6,7] who calculated the free energies of rectilinear vortex arrays of up to 30 vortices. It is predicted that the number of vortices present N will depend upon the rotation speed and diameter of the vessel. However, it is generally recognized that the existence of a large free energy barrier for the entrance of a vortex can lead to an immeasurably long lifetime for states with a different N than that of the equilibrium state. In Section 4 we discuss further the question of the equilibrium number of vortices and consider here only the properties of arrays of a given N.

Various configurations of rectilinear vortices that minimize the free energy F with respect to position variations have been calculated. One

finds that for some values of N several configurations exist which are local rather than absolute minima of F and as such are stable against small perturbations (such as thermal fluctuations). However, in an actual experimental situation, mechanical disturbances might be sufficient to cause transitions between different states. In the discussion which follows we use the term "stable (S) configuration" to designate the lowest energy pattern of a given N vortices. All higher energy patterns of the same N that are local minima in F will be referred to as "metastable (MS) configurations."

A feature which the S and MS configurations have in common is that they rotate as a unit with the walls of the vessel. This is a consequence of the form of the free energy expression for rectilinear vortices. However, such a state can only be attained if there exists a mechanism for the dissipation of excess free energy. Dissipation is known to occur when there is relative motion between the vortices and the normal fluid component, and is attributed to scattering between the vortices and the excitations comprising the normal fluid.[21] In the steady state, the normal fluid will rotate as a solid body with the vessel. Thus, in an experiment, vortices should be driven to an S or MS configuration through the action of the normal fluid. The process of energy dissipation is not limited to vortices that are straight. If prevented from assuming a rectilinear configuration (by pinning, for example), the vortices would be expected to assume whatever shape is required to produce solid body rotation of the cores, or be driven out entirely.

In this experiment, the positions of the cores of vortices at the free surface of the liquid are recorded by a camera which rotates along with the vessel. It is expected that any vortices present should appear stationary in this reference frame. In order to increase the rate of energy dissipation and thereby reduce the amount of time required for the attainment of the stationary state, a small amount (~0.8%) of ^{3}He impurity was added to the superfluid sample. Films were recorded over periods of many hours at constant angular velocity and reduced to multiple exposure prints (as discussed in Section 1). A sequence of such prints is shown in Fig. 3. The bright dots result from the repeated appearance of the vortex images at the same positions. Thus, the array is stationary.

In earlier work[8] with this apparatus the vortex positions could be recorded but stationary arrays were not observed. This was not due to any fundamental lack of stability for vortex systems in general. It may be that mechanical disturbances were so great as to overwhelm the feeble hydrodynamic interactions of the vortex system. As the vibration isolation of the cryostat was improved, stationary arrays became apparent. Those disturbances that remain seem to occur intermittently. This is illustrated by the blurred images in photograph 2 in Fig. 3. This particular form of blurring,

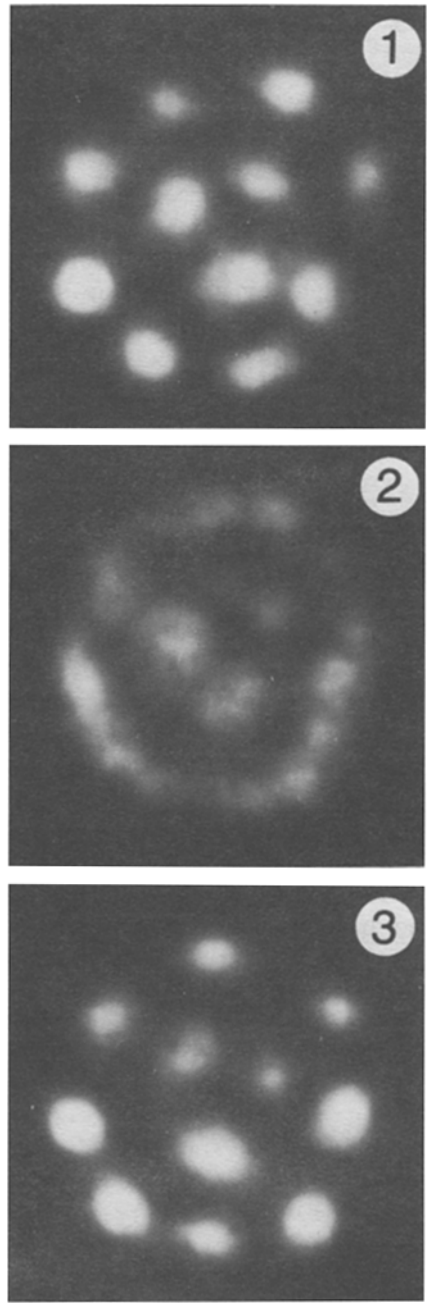

Fig. 3. A sequence of multiple exposure prints. Each print corresponds to 10.6 min of filming (60 frames) at a rotation speed of 0.59 rad/sec. Note the slight changes in the array configuration between photographs 1 and 3.

in the azimuthal direction, is the most common type observed. It is not unreasonable that this should happen since, at least for rectilinear vortices, rotations of a pattern arise from any slight change in the size of an array. Very little increase in free energy is required to produce a substantial change in the angular velocity of a pattern. (The net effect of a given disturbance would depend upon the rate at which this energy is dissipated.) The fact that arrays often keep the same orientation over periods of many hours seems to indicate that the lower ends of the vortices are pinned to the vessel.

Film records have been made at a variety of vessel rotation speeds, and stationary arrays of from 1–11 vortices have been observed. Multiple exposure prints of these were published in an earlier paper.[2] The observed patterns are similar to those predicted for rectilinear vortices, but some distortion from perfect symmetry is generally present. The deviations are greater than can be accounted for by optical distortion in the room-temperature part of the imaging system, and there is no systematic trend present that would suggest that other components (the electron optics and fiber optics) are at fault. Presumably the observed distortion arises from pinning of the vortices at surface irregularities on the bottom or side of the vessel. The fact that the distortion is usually slight might indicate that the pinning usually occurs near or at the bottom of the vessel. In our long and narrow vessel, the free ends would then be far from the regions of high vortex curvature, and their positions might tend to reflect the interactions of rectilinear vortices.

For the most part, the observed patterns can be identified with the predicted S configuration for that particular number of vortices. In the case of six lines, however, two distinct configurations are observed. One corresponds rather closely with the S configuration and the other with the MS configuration. These arrays appeared alternately during a 5-h period at constant rotation speed. The series of multiple exposure prints shown in Fig. 4 is taken from this film and shows one of the transitions between states which occurred. The details of the transition cannot be discerned from the film. The two states last for varying amounts of time ranging from as long as 1 h to as short as 2 min. (This is roughly the amount of time required for a pattern to stabilize.) The predicted S and MS configurations are also shown in Fig. 4 for comparison. MS configurations are also predicted for 5, 9, 10, and 11 vortices, but none of the observed patterns show any close correspondence with these configurations. However, in the case of 10 lines the difference between the S and MS configurations is so slight (basically a rotation of the inner two vortices relative to the outer ring) that no obvious distinction could be detected in this experiment. The other S and MS configurations involve different numbers of interior and exterior vortices, as do those of six lines.

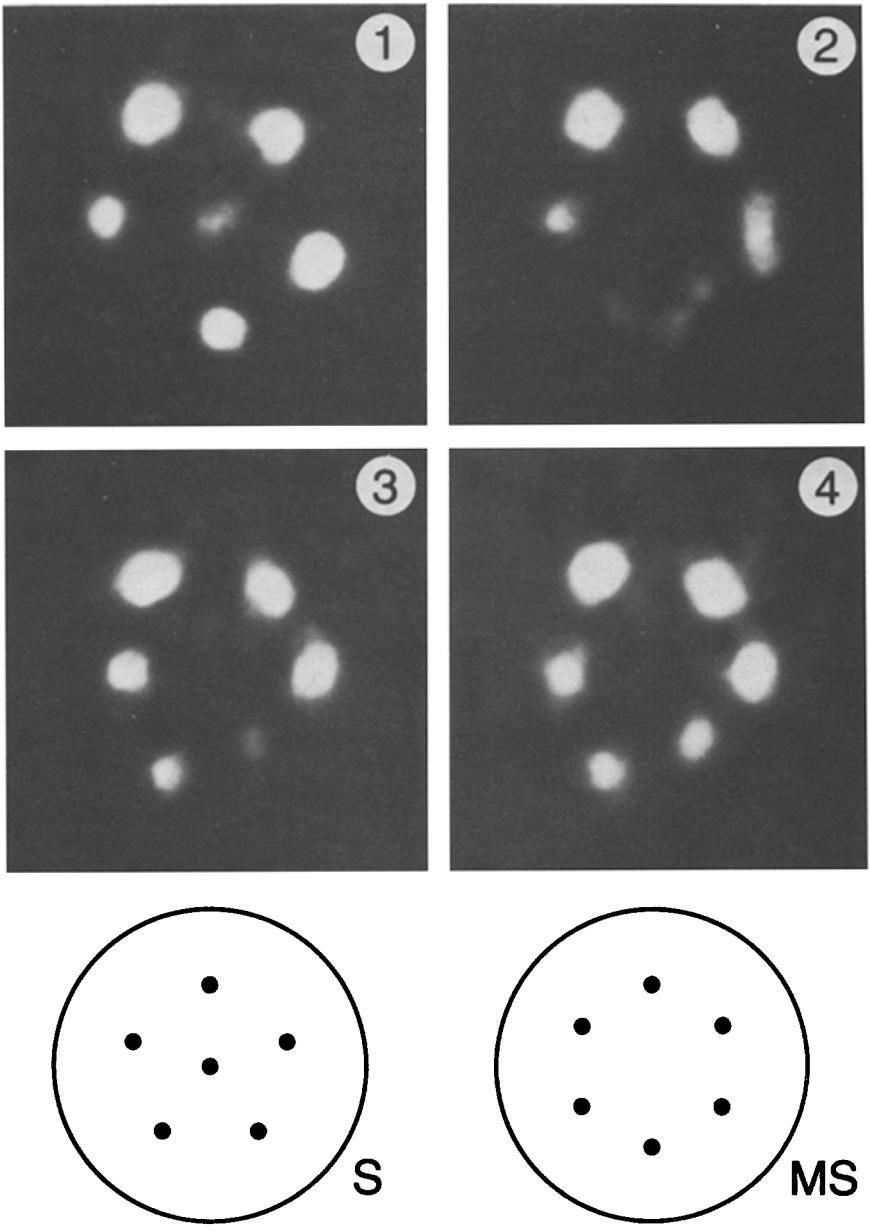

Fig. 4. Photographs 1–4 are sequential multiple exposure prints. These are 30-frame exposures and each corresponds to 6.7 min of filming at 0.47 rad/sec. Below these are shown the predicted S and MS configurations for a rectilinear array of six vortices as given in Ref. 8.

Not all of the observed stationary patterns appear as slightly distorted versions of those predicted for rectilinear vortices. Examples of some of these unusual arrays are shown in Fig. 5. These occur rather infrequently

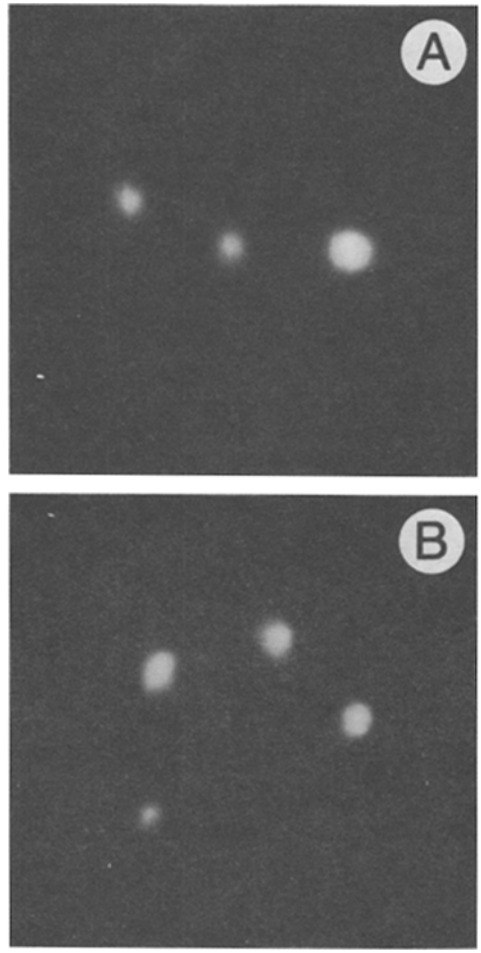

Fig. 5. Multiple exposure prints showing some unusual array configurations. Photograph A is a 60-frame exposure corresponding to 10.6 min of filming at a rotation speed of 0.42 rad/sec, and photograph B is a 30-frame exposure corresponding to 7.9 min of filming at 0.40 rad/sec. The predicted S configuration for three lines has the vortices located at the corners of an equilateral triangle, and for four lines the vortices are at the corners of a square.

and may be due to pinning of lines at points near the free surface of the liquid. In some cases the observed pattern would appear similar to a predicted S configuration if only an additional vortex were present. In Fig. 5b, for example, a good approximation to a pentagonal array can be produced by adding one extra image. In fact, in this particular example, a pentagonal array was observed just prior to the appearance of this distorted four-line pattern (at constant rotation speed). It may be that a mechanical disturbance caused the fifth line to bend over and become attached to the side of the vessel. If such were the case, its image would not be recorded but its presence would be felt by the other line. Another possibility is that a vortex could escape detection by being located beneath one of the regions of poor transmission in the image conduit (see Fig. 2). In fact, it is often the case that an image which appears weak in the multiply exposed prints is a result of a consistently dim image on the film rather than motion of the image from frame to frame. Such instances of partial light loss would be expected for this image conduit. (A line which is short by virtue of its lower end being pinned to the wall could also produce a dim image because it would trap less charge than other, longer lines.) The fact that most of the observed patterns retain their apparent vortex number following disturbances and slight repositionings of the vortices indicates that long-term image loss in the image conduit occurs infrequently enough to not present a substantial problem. Of course, vortices that do not appear because they are either too short or do not reach the surface are an ever-present possibility.

Multiple exposure prints are not required for the observation of stationary arrays. Because they are stationary, the vortex images stand out among the general background of noise from the image intensifier when the films are projected at 18 frames per second. In films recorded with the optimum television gain settings, it is seldom that a noise flash appears in the region of interest, and the arrays can be discerned in individual frames. Examination of these shows that the images fluctuate in intensity and are occasionally missing entirely. This is illustrated by the series of individual film frames shown in Fig. 6. Note that an image that is missing in one frame subsequently reappears at the same location. Note also that there is no apparent response of the array as a whole. It seems highly unlikely that this would occur if the vortex had actually disappeared or moved significantly. A more likely explanation is that the image loss is due to an imperfection in the apparatus. This problem varies in its severity and often affects particular members of an array more than others. Usually a given vortex image is missing in about 15% of the film frames, but this may be less than 1% or as high as 90%. (The identification of an array member involves the repeated observation of an image within a small area on the

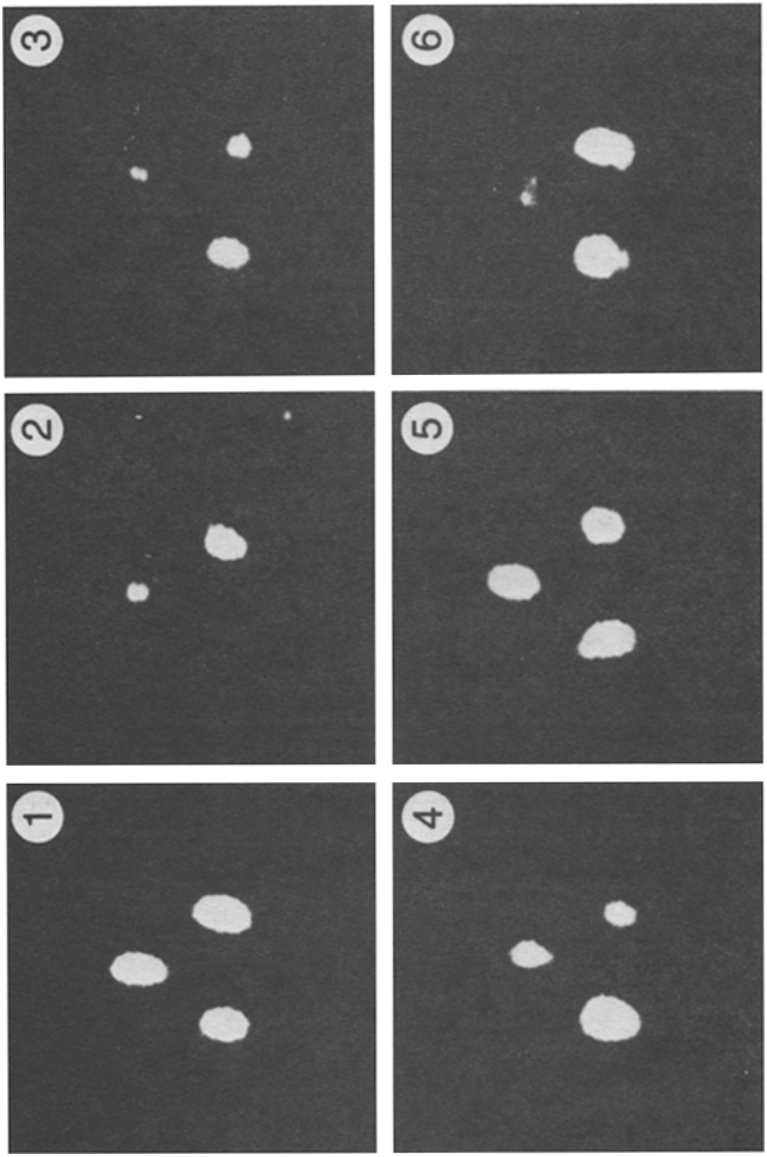

Fig. 6. A sequence of single-frame photographs recorded at a rotation speed of 0.40 rad/sec. The time between frames is 15.6 sec. Large fluctuations in the image intensities (and sizes) can be seen.

film and the probability that a noise flash would occur there more often than once or twice in several hundred frames is extremely small for those films studied.)

Since the intensity and size of the images vary considerably from frame to frame, it is reasonable to suppose that the missing images simply correspond to those that have dropped below the threshold for detection on the film. Such a fluctuation might occur if a line were to move slightly and pass beneath a region of poor transmission in the image conduit. It might also be that clumps on the phosphor screen reduce the amount of locally transmitted light or that the total trapped charge fluctuates (though with several thousand ions trapped, statistical fluctuations should be small). It is interesting to note that even a significant transient image loss (such as both members of a two-line array) usually produces no noticeable decrease in the amount of light received over the whole of the fiber optics. (These light measurements do not interfere with filming and are described in section 4.) This suggests that diffuse scattering rather than the actual loss of light may be responsible for this effect. Although doubts remain as to the precise cause of this problem, the fact that the arrays are unaffected provides a strong justification for considering this to be a mere nuisance rather than a serious problem. However, for arrays of more than about five vortices almost every frame lacks one or more image. Thus, a practical limit is imposed which prevents the detailed, frame-by-frame study of arrays of many vortices.

Generally speaking, we find qualitative agreement between the observed stationary patterns and those predicted for rectilinear vortices. Thus we are prompted to consider the extent of any quantitative agreement. According to rectilinear vortex theory, the size of any stationary configuration depends upon the rotation speed, the number of vortices, and the circulation of each vortex.[9] In an unbounded fluid, a stationary array of N singly quantized vortex lines will satisfy

$$\sum_{j=1}^{N} r_j^2 = \frac{h}{m} \frac{N(N-1)}{4\pi\Omega} \tag{1}$$

Here r_j is the distance of the jth vortex from the axis of rotation of the pattern, Ω is the rotation speed at which the pattern appears stationary, h is Planck's constant, and m is the mass of a helium atom. This is only an approximation if the fluid is bounded, but unless the vortices are very close to the boundary the approximation is very good.

In order to apply this equation to the observed patterns, a choice must be made for the origin to be used in measuring the r_j. We cannot use the

axis of the vessel, because its location is not accurately known. The 2-mm-diameter vessel is mechanically aligned so as to be approximately centered beneath the 3.2-mm-diameter image conduit, but no direct determination of its position was made during the experimental run. The location of the axis of rotation of the apparatus is even less well known, and quite possibly lies outside of the vessel. However, as long as the observer's rotation axis coincides with that of the apparatus (it does), the normal fluid (and hence the vortices) should appear stationary when dissipation has ceased. If the vortices were rectilinear, the patterns would be expected to display perfect cylindrical symmetry and be centered on the axis of the vessel. The choice of axis for the measurement of the r_j would therefore be determined by the pattern itself and would correspond to an origin such that $\sum_{j=1}^{N} r_j^2$ is minimized. We make the assumption that, for the observed patterns, the relevant origin is the one that minimizes this sum. Any error arising from this assumption can be considered to arise from array distortion (unless some of the vortices are multiply quantized).

Using Eq. (1) to extract a "quantum of circulation" from the observed patterns, we find values in rough agreement with the accepted value of h/m. Measurements of four- and five-line arrays (which are quite symmetric) yield values which agree within 5%. In fact, two different four-line arrays at rotation speeds more than a factor of two apart give such agreement. Some of the more distorted patterns give results which differ by as much as 30%. While there appears to be some correlation between the amount of distortion and the magnitude of the discrepancy, this trend has not been firmly established. As a counterexample of this, the nearly perfect 11-line array shown in Fig. 3 yields a value of h/m which is 20% low.

Because of the transient image losses, the measurement of most of the patterns must be made on the multiply exposed prints. Much information is lost in the process. In particular, the amount of motion of the vortices cannot be accurately determined. For this reason, we have concentrated our efforts on an array which can be studied in detail, that of two lines. The simplicity of this array eliminates all subjective judgements involving distortion. As mentioned in Section 1 one of the methods of data collection involves the filming of sequences of spinups to a particular final rotation speed. One such sequence (with a final rotation speed of 0.364 rad/sec maintained for periods of 1 h) resulted in the appearance of a stationary two-line array in almost every trial. (The others had stationary one-line arrays.) Portions of the film records of 18 of these trials were digitized using a film scanner, and the vortex pair separation was measured for each frame. (Some frames have only one image present and were skipped.)

Plots of the pair separation versus frame number for two successive trials are shown in Fig. 7. Between trials, the vessel was at rest for 1 h.

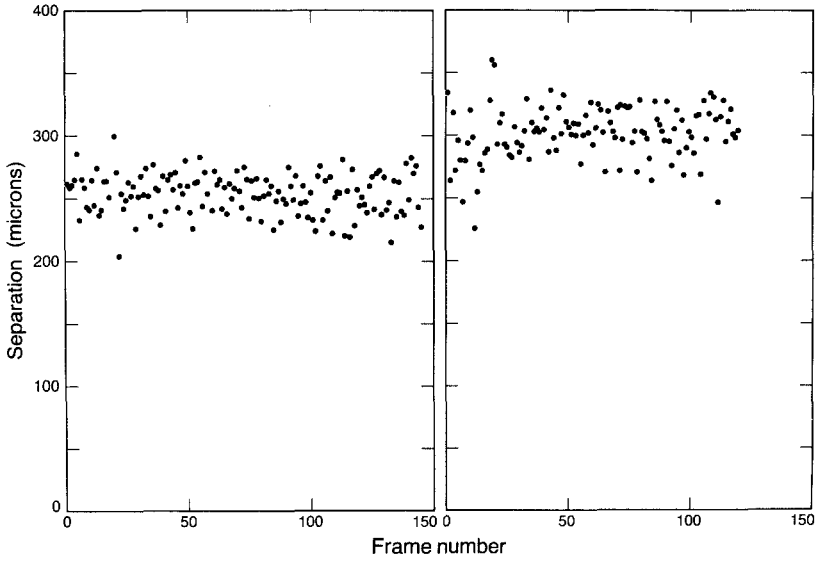

Fig. 7. The separation of the vortices in a two-line array plotted vs. film frame number for two successive spinup trials. The rotation speed was 0.364 rad/sec for both. The time between film frames was 10.6 sec.

The separations are measured between the centers of the two images, the positions of which are judged using the crosshair of the film scanner. The scatter in the measured separations of a given trial (the standard deviation) is approximately 20 μm somewhat smaller than the typical individual vortex image diameter of 100 μm. Distances on the film have been converted to those that occur at the fluid surface using the overall image magnification. There is a possibility that the image diameters are increased as a result of flaring in the room-temperature part of the optical system. Fiducial images, produced by two pinhole light sources attached to the television monitor, are present in each frame, and allow frame-to-frame comparisons of the vortex image locations. The measured positions have a scatter (in the x or y coordinate) of 15 μm. The errors made in the judgement of the image centers are estimated from repeated measurements of a group of frames and found to be 10 μm. Thus, the image displacements are approximately equal to the measurement errors. It is interesting to note that the diameter of an individual fiber in the image conduit is 11.6 μm.

There is a clear difference between the average separations for the two spinup trials shown in Fig. 7. Figure 8 is a plot of the average separation for all 18 of the trials. The error bars on the points are the standard deviation of the mean as determined from the individual frame measurements. The large scatter in the mean separations is apparent. The solid

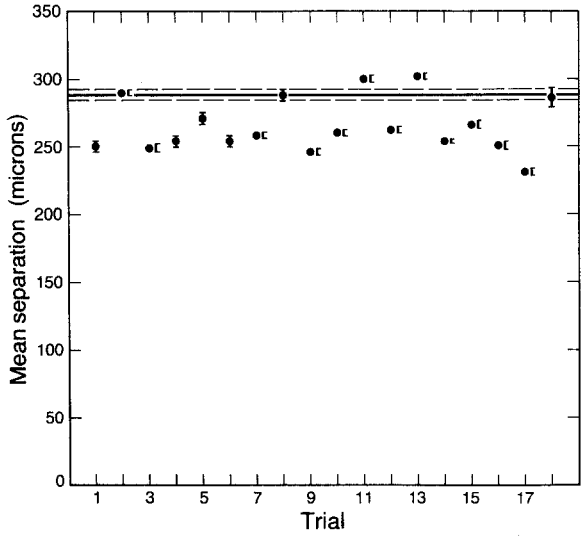

Fig. 8. The time-averaged separations of the vortices in two-line arrays produced by independent spinups to a rotation speed of 0.364 rad/sec. The data are plotted vs. the spinup trial number (chronologically ordered). The solid line is the predicted separation for rectilinear vortices and the dashed lines indicate the uncertainty in this prediction as explained in the text.

line is the predicted separation using Eq. (1) and the accepted value of h/m. The systematic error from the uncertainty in the overall image magnification is indicated by the dashed lines above and below the solid line.

Since the vortices in this experiment are probably not simple rectilinear structures, close quantitative agreement with rectilinear vortex predictions cannot be expected. While scatter in the measurements is not surprising, it is not obvious that the two-line array separations should tend to be smaller than predicted. Another trend in the two-line data is the clustering of the angular orientation of the stationary states about a particular value. Of the 18 trials, 17 have angular orientations within a spread of 75 deg. One would expect a spread of 180 deg for a random distribution. No apparent correlation is observed between the orientation angle and the separation of the pair.

3. ARRAY OSCILLATIONS

The motion picture film records show the positions of the vortices at the free surface as a function of time and thus contain information about

the dynamic as well as static properties of arrays. Useful dynamical information can only be obtained if the vortex velocities are small enough so that displacements which occur in the time between photographs are less than the intervortex spacing. In such cases it becomes possible to follow the motion of particular members of an array. Throughout most of the film sequences, the arrays appear stationary, and even though particular vortices can be identified over long periods of time, their motion appears random and is approximately equal to the spatial resolution of the system. Occasionally, however, distinct periodic motion is observed.

One type of oscillatory motion appears as a transient preceding the establishment of stationary two-line arrays. As mentioned in the previous section, sequences of spinup trials were recorded in which a two-line array usually appears. Following the acceleration of the vessel, a particular sequence of events is usually observed. Approximately 7 min after the final speed is reached (0.364 rad/sec for the sequence studied) a single vortex appears and settles down to a stationary position within a few minutes. No simple trajectories can be followed for this first vortex. The motion appears chaotic but with an amplitude which decreases with time. A second vortex appears after another 10–20 min (though in some instances a single line remains for the full hour of rotation). Initially the two lines move about rapidly, but after several minutes the motion decays to the point where individual trajectories can be discerned. During this final approach to equilibrium, the two vortices often exhibit a damped azimuthal oscillation about their common center.

Three trials have been analyzed in detail. A film scanner was used to determine the locations of the images in each frame, and from this the angular orientation of the pair was calculated. This is the angle between a fixed reference line and the line joining the vortices. The reference line was chosen in each trial so that the equilibrium orientation angle is approximately zero. A problem with the analysis of such single-frame data is that images are missing in some of the frames. As mentioned in the previous section, this seems to be due to fluctuations in the image intensity rather than the disappearance of a vortex. Approximately 17% of the frames have one member of the pair missing. In these cases the angle was estimated from the position of the one image present and the time-averaged midpoint location of the pair. Roughly 2% of the frames have both images missing and allowed no determination of the orientation. Plots of the orientation angle versus time are shown in Fig. 9. Angles that were estimated on the basis of a single image are shown as open circles. The decaying oscillations of the angular orientation are apparent. Plots of the midpoint location and the separation of the two vortices show no such obvious periodic behavior. These display random variations with a magnitude only slightly greater

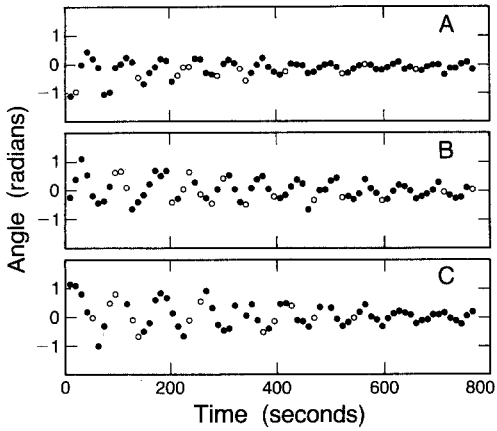

Fig. 9. The angular orientation of two-line arrays plotted vs. time for three different spinups, all to a rotation speed of 0.364 rad/sec. The open circles are points determined on the basis of a single vortex image as discussed in the text.

than that observed for stationary arrays. Figure 10 shows transient C of Fig. 9 replotted together with a sequence of prints from the individual frames of the motion picture record. The sequence of prints corresponds to the region of the angular plot that is denoted by arrows.

The transients were fit to exponentially decaying sinusoidal oscillations. The mean squared deviation χ^2 decreases sharply and then levels off as more of the high-amplitude points are left out of the fit. For transients A and B, χ^2 is constant for starting amplitudes (peak to peak) that are less

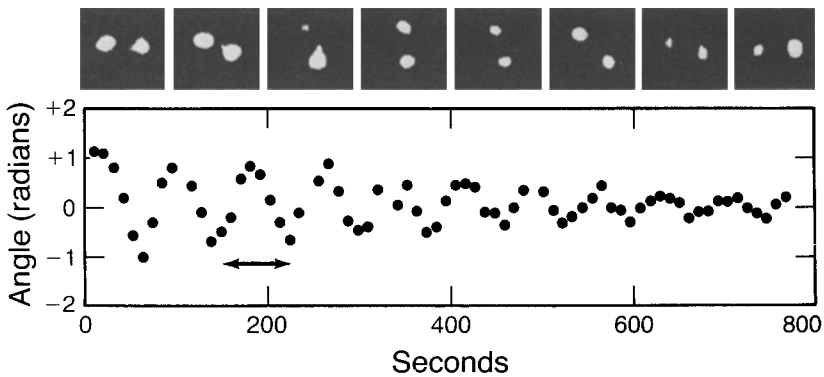

Fig. 10. Transient C of Fig. 9 replotted together with a segment of the motion picture film sequence. The arrows indicate the portion of the angular plot corresponding to the photographs.

than 1.0 rad (about the 15th point in the figure). It can be seen that the early portions of these transients show a smooth change in the average orientation angle (upward curvature in A, downward in B). Because such a baseline drift was not included in the fitting function, the inclusion of the early portions greatly increases χ^2. For transient C, the leveling off of χ^2 occurs at an amplitude of about 1.5 rad (tenth point). No clear baseline drift is present and it may be that the breakdown of the fit reflects a growing importance for nonlinear effects at large oscillation amplitudes. The choice of starting point has very little effect upon the fitted values of the oscillation frequency. The frequencies are 0.100, 0.095, and 0.083 rad/sec for A, B, and C, respectively, and have uncertainties of 1%. The fitted decay times are more sensitive to the choice of starting point, but, like the mean squared deviations, these level off as more of the initial points are excluded. After leveling off, the fitted decay times are 400, 380, and 370 sec for A, B, and C, respectively, and have uncertainties of about 20%.

Azimuthal oscillations were also observed for an array of four vortices. However, in this case, the motion occurred at intermittent intervals throughout a constant rotation speed (0.400 rad/sec) filming sequence. These do not appear to be related to any identifiable perturbation of the vortex system (such as the entrance of a vortex) and do not have the form of a decaying transient. A portion of the film sequence was analyzed in a manner similar to that described above for the two-line data. The center location of the array was calculated by averaging the positions of the four images, and lines between this point and each of the images were determined. The overall angular orientation was calculated by averaging the polar angles of these four lines. About 25% of the frames have one or more of the images missing (most often only one). In these cases the angle was estimated by adding a point at a location which completes the square array. A plot of the orientation angle versus time is shown in Fig. 11.

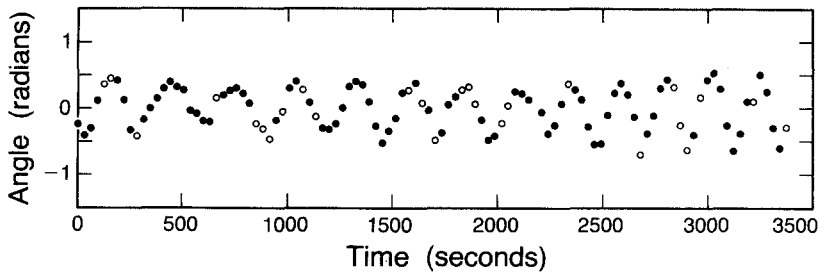

Fig. 11. The angular orientation of a four-line array plotted vs. time. The data were obtained at a rotation speed of 0.400 rad/sec. The open circles are points estimated on the basis of fewer than four images as discussed in the text.

Thirteen complete cycles occur over a period of about 3300 sec. The average oscillation frequency is therefore 0.024 rad/sec. However, the frequency appears to be increasing with time, varying from about 0.021 to 0.029 rad/sec. The reason for this variation is not known. Plots of the center location and radius of the array show no apparent periodic behavior.

A more complex motion has been observed for an array of three vortices. In this case three distinct types of oscillation appear simultaneously. There is motion of the center of the array, azimuthal motion about the center, and motion involving a distortion of the array shape. All three types appear throughout the film record of a 22-h constant-rotation-speed (0.400 rad/sec) trial. A portion of this film was digitized and the data were computer-analyzed in order to separately examine the various aspects of the motion. The center position of the array is calculated by averaging the measured positions of the three vortex images. The angular orientation is determined by averaging the angular positions of the three images relative to a coordinate system which has its origin at the calculated center point of the array. Out of the 740 frames measured, 9% have one image missing and 1% have two missing. For these frames the angular orientation is estimated on the basis of the images present, using the locally time-averaged center position of the array as the coordinate origin. The remaining component of the array motion (that which results in a distortion of the configuration) is evaluated by means of a coordinate transformation applied to each frame. The Cartesian coordinates of each image are determined relative to the center position of the array (thus removing center motion) and then are rotated by the negative of the calculated orientation angle (thus removing angular motion). Transformed in this way, the image coordinates reflect only the distortive component of the array motion. (Variations in the size of the array would remain, but this quantity displays no obvious periodic behavior.) The time dependence of the center position of the array is shown in Fig. 12A. The center moves about a highly elliptical orbit (major axis $\approx 10 \times$ minor axis) and only the projection on the major axis is shown in the figure. Motion of this type is known to arise from the rotation of the magnetically focused television camera through the earth's magnetic field. The entire television image is shifted about in synchronism with the rotation of the apparatus. In this particular film sequence the time between film frames (15.586 sec) is slightly less than the time required for a complete revolution of the apparatus (15.71 sec). This slight difference in timing results in an apparent motion which is stroboscopically reduced in frequency from 0.400 to 0.0032 rad/sec. The observed center motion occurs at a frequency of 0.0025 rad/sec. Given the uncertainty in the measured rotation speed (0.5%), these are in agreement. The amplitude of the displacement is also approximately equal to that measured for a test

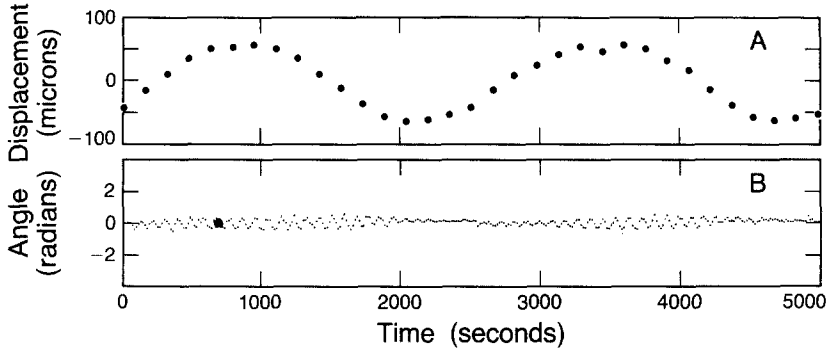

Fig. 12. The time dependence of (A) the center position and (B) angular orientation of a three-line array. The center position is averaged over groups of ten frames and the projection of its displacement along one axis (see text) is plotted. The data were obtained at a rotation speed of 0.400 rad/sec.

pattern recorded by the rotating camera. Thus, the observed center motion of the array cannot be attributed to actual motion of the vortices. This spurious effect was avoided in most of the films recorded early in the experimental run by carefully matching the filming cycle to the rotation speed (this was the case for the four-line oscillations). For the film of the three-line array a slight error in timing was made. Later in the run the spurious motion was removed entirely by means of a pair of large magnet coils which canceled the earth's magnetic field. This allowed filming at any convenient time interval. The films showing azimuthal oscillations of two-line arrays were recorded with these coils in operation.

Figure 12B shows a plot of the angular orientation vs. time for the three-line array. The measured oscillation frequency is 0.068 ± 0.001 rad/sec and appears to be constant throughout the sequence.

The motion that remains after azimuthal and center motion are subtracted is illustrated in Fig. 13A. Each of the plotted points represents the position of a vortex averaged over ten film frames. The motion is periodic and the points shown correspond to four complete cycles of the vortices about the somewhat elliptical orbits. The varying density of points along the orbits is due to the fact that the motion is not uniform in time. The film record shows that this motion persisted for at least 22 h and appears at the same frequency as the motion of the array center. It seems likely that the apparent motion has been stroboscopically reduced and has an actual frequency equal to that of the rotation speed. Although this suggests that the cause of the periodic distortion may simply be some type of instrumental effect which is associated with the rotation of the apparatus, no such mechanism has been found. Films of a test pattern made while

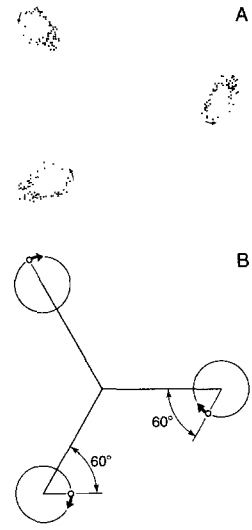

Fig. 13. (A) The measured distortive motion of a three-line array and (B) the predicted normal mode motion for rectilinear vortices. Each point in A is the average of ten film frame image locations after azimuthal and displacive motion have been subtracted out (see text). The arrows in A and B indicate the sense and the relative phases of the orbital motion. The data shown are for four complete cycles of motion. The predicted normal mode motion (B) includes the effects of a finite cylindrical boundary, and the orbits are elliptical rather than circular. However, the effect is too small to be seen in this plot.

rotating show no such periodic distortion. Of course, we cannot rule out the possibility that some more subtle effect is responsible. For instance, there may be a periodic distortion occurring as a result of a problem associated with the low-temperature electron optics which would not show up in a test of the room-temperature part of the system. However, other films recorded with a slight difference between the film cycle time and the rotation period show only the slow periodic translation of the arrays; no periodic distortion is observed.

A puzzling feature of the observations is that the distortive oscillations persist without apparent decay for a very long period of time (22 h). If the observations are actually due to vortex motion, a driving force would have to be present in order to maintain the oscillations. It is possible that mechanical perturbations arising from the rotation of the apparatus could couple into the vortex system and produce a response at the frequency of rotation, but we have no direct proof that such is the case.

Another curious feature is that the three-line azimuthal oscillations seem to be connected in some way with the other components of the motion. It can be seen from Fig. 12B that the intervals of oscillation occur regularly with a period equal to that of the stroboscopically slowed center or distortive motion. As with the distortive motion, no instrumental effect has been found that results in azimuthal oscillations of the images. Furthermore, the appearance of such oscillations in the case of two-line arrays appears to be causally related to a definite perturbation of the vortex system (the entrance of an additional vortex). This relation seems to indicate that

the phenomena of azimuthal oscillations is a real effect arising from actual vortex motion. It is difficult to imagine what connection there could be between the azimuthal oscillations and the spurious image motion arising from the television camera. One might be able to construct a model for an interaction between the distortive motion (if it is not spurious) and the azimuthal oscillations, but we have been unable to find one simple enough to be considered likely.

The observed orbits of the three vortices (Fig. 13A) are actually quite similar to those predicted for one of the normal modes of an array of three straight vortices. Calculations of the motion of such an array were first performed by Lord Kelvin[10] and were later extended by Havelock[11] to include the effects of a finite cylindrical boundary. Figure 13B shows a plot of the orbits for one of the three normal modes predicted for such an array. The orbits have been calculated* for a vessel of diameter 0.2 cm and a rotation speed of 0.400 rad/sec (the same as the experimental conditions). Comparison with Fig. 13A reveals the similarity between the predicted and observed motions. In both figures the orbits are shown for the sense of vessel rotation being counterclockwise. (Inversions of the image in the optical system have been accounted for in the experimental data.) At first sight it appears that the observed orbital motion occurs in a sense opposite to that predicted. However, a reversal of the sense of the motion is expected to occur for periodic motion at the rotation frequency of the vessel because of the stroboscopic frequency reduction effect. (Had the time between film frames been greater rather than less than the period of revolution, motion occurring at the frequency of rotation would have appeared slowed, but not reversed.) In the absence of boundaries, the predicted frequency of the motion shown in Fig. 13B is equal to the rotation frequency. The effect of a cylindrical boundary is to reduce the frequency by an amount that depends upon the size of the vessel relative to the size of the array. Under the conditions of this experiment this frequency would be expected to be 0.991 times the rotation frequency.

Even this slight reduction would give rise to a very noticeable difference in apparent frequency between distortive mode motion and the array center motion (believed to be at precisely the rotation frequency). This is not observed. However, if such motion were to be driven by external perturbations, the response would be at the drive frequency and would have an amplitude determined by the amount of drag present.

One feature of the data is in sharp disagreement with the theory. This is the nonuniformity of the orbital motion. Since the orbital amplitudes are quite small compared with the vortex separations, it seems unlikely

*The calculation was made using the results in Ref. 11. We included the correction to Eq. (25) pointed out in Ref. 12, footnote 19, p. 158.

that nonlinear interactions would be strong enough to produce substantial nonuniformity. It is possible that regular variations in the angular velocity of the apparatus could produce such an effect, but these would be expected to show up in the apparent center motion as well. The smooth sinusoidal variations of the center position (Fig. 12A) show no hint of such nonuniformity.

Two other normal modes are predicted for an array of three vortices. One of these involves a translation of the array as a whole and would appear as motion of the center of the array. The frequency of this mode is strongly affected by the presence of a cylindrical boundary. It is equal to the rotation frequency in the absence of a boundary but is reduced to 0.881 times the rotation frequency for conditions as in this experiment. This displacive type of motion is indistinguishable from that produced by the rotating television camera, except for the fact that, at resonance, its apparent frequency would be different. All observed motion of this type can be attributed to the known instrumental effect.

The remaining normal mode is similar to the observed azimuthal type of motion in that it involves azimuthal displacements of the vortices. However, the predicted oscillation frequency is zero (with or without a cylindrical boundary). This particular type of mode is common to all stable vortex arrays and arises in the following manner. Consider the response of a stable array which initially is stationary as viewed by a rotating observer. A slight change in the size of the array will result in a uniform rotation of the array at an angular velocity which is proportional to the change in the dimensions of the array (the size of an array determines the rotation speed at which it will appear stationary). If no drag were present, the rotation of the array would continue indefinitely. In a normal mode analysis this corresponds to a mode with zero frequency because the response (the angular orientation of the array) grows linearly with time. Even if drag were present (as would be the case in an experiment) it would only cause a decay of the motion and the real part of the mode frequency would still be zero.

The observed azimuthal oscillations cannot be explained in terms of rectilinear vortex motion. However, real vortex systems are not restricted to motion in only two dimensions. In fact, if the ends of the vortices are pinned at surface irregularities at the bottom of the vessel, an azimuthal displacement of the vortices at the free surface would have to involve bending of the lines. The rectilinear vortex model is incapable of describing such a situation. Calculations of the response of vortex arrays to three-dimensional perturbations have been carried out for the limiting case of a dense array[13] and for an isolated vortex.[14,15] These have been successfully used for the interpretation of observed vortex wave phenomena in arrays

containing many vortices[16,17] and in a situation where collective effects are unimportant,[18] but they cannot be directly applied to this experiment. In the case of the dense array, a continuum description is used in which only first-order contributions arising from the discrete nature of the array are included. Of course, with only a few vortices present, the discreteness of the array is critically important. In the opposite limit, that of an isolated vortex, collective effects arising from the interaction between vortices are nonexistent. Ignoring these would be an oversimplification for arrays of more than one vortex.

A generalization of the three-dimensional isolated vortex model to include interactions among a small number of vortices might be expected to provide an adequate description of real arrays. We have performed such calculations for the specific cases of two-, three-, and four-line arrays. Their details will be presented in a future paper. Basically the effect of including vortex flexure is to increase the frequencies of all modes. In the long-wavelength limit, those modes that have frequencies of the order of the rotation frequency in a two-dimensional treatment are increased by an amount proportional to the square of the wave vector. Provided the wavelength is not much smaller than the vortex separation, the frequency change is small. The effect of vortex flexure upon the azimuthal modes (which have zero frequency in the 2D limit) is found to be much greater. The addition of flexure leads to a finite frequency which is proportional to the first (rather than second) power of the wave vector. To the lowest order in the wave vector k, the predicted azimuthal oscillation frequencies for $N = 2$, 3, or 4 lines are given by

$$\omega = k\left[\frac{\Omega h}{2\pi m}\ln\frac{b}{a}+\frac{N-1}{2}\right]^{1/2}$$

Here, h is Planck's constant, m is the mass of a helium atom, Ω is the rotation speed, a is the vortex core parameter, and b is the vortex separation (for four lines, the diagonal of the square).

In order to make a quantitative comparison with the measured frequencies, the wavevector must be specified. If the vortices are assumed to be pinned at the bottom and free at the top, a reasonable estimate of the wave vector would be that which satisfies a resonance condition in which an odd integral number of quarter wavelengths fit within the height of the vessel (22.7 mm). For this choice, the predicted fundamental mode frequencies are 0.0206, 0.0221, and 0.0227 rad/sec for two-, three-, and four-line arrays, respectively, where we have used the values of the rotation speed at which the oscillations were observed (0.364 rad/sec for two lines, 0.400 rad/sec for three and four lines). A value of 1.0 Å was used for the

vortex core parameter. The measured frequencies are 2–5 times greater than these predictions.

In judging this comparison, a number of factors must be considered. First, there is no reason to expect oscillations to occur only at the fundamental frequency. Since the length scale of the fluid disturbances is not known, one cannot assume that only the longest wavelength mode would be excited. Second, there is the effect of the fluid boundary condition at the vessel bottom. Since a vortex must come in perpendicular to a solid boundary (at least on some length scale), the lower ends of the lines cannot be nodes of purely sinusoidal deformations. However, if pinned, they would be unlikely to be antinodes either. The same problem is encountered in experiments involving dense arrays of vortices. In such an experiment, Andereck *et al.*[17] find good agreement with continuum vortex theory using a resonance wavelength criterion similar to that we have assumed. (Having solid walls for both the upper and lower boundaries, they take the bending wavelength to be twice the boundary separation.) Some of the more subtle, boundary-related aspects of the continuum vortex model have been considered by Sonin.[19]

The most important factor to consider when making a quantitative comparison is that the vortex configurations may be far from rectilinear. Even though flexure has been included in the theoretical model, only small deviations from an otherwise rectilinear array are assumed to be present. The effects of significant steady state vortex curvature cannot be easily accounted for. Even if steady state curvature is ignored, there is still the possibility that the vortices are pinned to the side and do not reach the bottom of the vessel. Shorter vortices would have smaller resonant wavelengths and hence higher oscillation frequencies. Matters would be further complicated if the vortices each had different lengths. In light of these experimental uncertainties, the discrepancies between the measured and predicted frequencies are probably not significant.

We have also used this theoretical model to predict the decay times of transient oscillations in terms of the drag force experienced by the vortices in moving through the normal fluid component. At the low temperature required for this experiment (0.1 K), the drag arises mainly from the scattering of ^{3}He impurities by the vortices. Approximately 0.8% ^{3}He was added to the superfluid sample in order to provide this type of drag. One can compare the measured decay times of the transient two-line array oscillations with that expected on the basis of the vortex ring energy-loss measurements of Rayfield and Reif.[20] In order to do this, the measured drag force (at 0.0028% ^{3}He and 0.28 K) must be adjusted to account for the higher ^{3}He concentration and the lower temperature of this experiment. Rayfield and Reif show that the drag force should be proportional to the

number density of ^{3}He atoms and to the square root of the temperature. Scaling the drag force in this way and including it in the vortex equation of motion for the two-line model, we find that the decay time should be approximately 500 sec (and does not depend on the wave vector if the wavelength is long). This agrees within 30% with the observed decay times.

A more refined estimate of the decay time from the vortex ring data would have to include some of the more subtle aspects of the ^{3}He scattering problem. For example, spin statistics should become important when the Fermi energy of the ^{3}He quasiparticles is nearly equal to their thermal energy. This is the case in this experiment, but not in the lower concentration vortex ring studies. Also, as Hall and Vinen point out,[21] there is a hydrodynamic correction which must be applied to calculations of the drag in order to account for the dragging of the quasiparticles in the vicinity of the vortex core. This correction is expected to become significant at very low vortex velocities as in the case of these low-frequency vortex waves. The condensation of ^{3}He atoms onto the vortex cores[22] might also result in measurable drag force changes. In addition, changes in the vortex core structure resulting from this condensation would be expected to alter the wave speed and hence the resonant frequency of the oscillations. We have not attempted to include these refinements in an estimate of the decay time. These are mentioned only to point out the rough nature of the present estimate and to indicate the classes of phenomena which can, in principle, be probed using this photographic technique.

One further point concerning the predicted azimuthal modes is that the motion involves changes in array radius as well as rotation about the center. The observed lack of obvious radial oscillations is not inconsistent with this, because the predicted radial component is very small. In the limit of long wavelengths, the ratio of the radial to angular amplitudes (δr and $\delta\theta$) is given by

$$\delta r/\delta\theta = r\omega/2\Omega \tag{2}$$

where r is the array radius, ω is the oscillation frequency, and Ω is the rotation speed. For the observed oscillations, δr is expected to be 20 μm or less. This is only slightly greater than the measurement errors ($\sim$10 μm). However, peaks of approximately the expected size are present in Fourier transforms of the three- and four-line oscillation data. Figure 14 shows the frequency spectra for both the radial and angular components of each data set. The plots are the square root of the noise power spectra, and have been scaled according to Eq. (2) so that each radial spectrum should have a peak of the same magnitude (and frequency) as that of its corresponding angular spectrum. In scaling the spectra we used the measured array

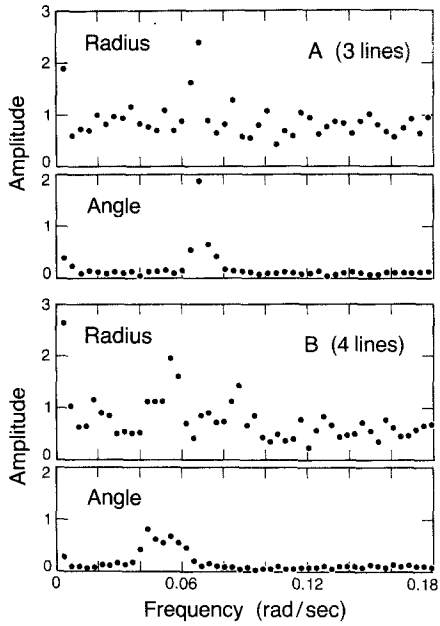

Fig. 14. Frequency spectra for the radius and angular orientation of (A) three-line and (B) four-line arrays that showed clear azimuthal oscillations. The relative vertical scales have been adjusted as described in the text, but otherwise the amplitude units are arbitrary.

radii and oscillation frequencies (rather than the predicted fundamental frequencies). Fourier transforms of the two-line transient oscillations show clear peaks for the angle data but the spectra for the radius data are dominated by noise. Although peaks in the spectral amplitudes are discernible for the three- and four-line data, the noise is too large to allow measurement of the relative phases between the radial and angular oscillations (expected to be 90°).

4. SPINUP PHENOMENA

The free energy barrier which must be overcome by vortices entering a vessel has been shown to be very large compared to kT if the vortices are constrained to be rectilinear.[6] It is so much higher than typical thermal energies that thermal nucleation of fully developed vortices should virtually never occur. Of course, real vortices are not constrained to be straight, and it has been suggested that the barrier energy might be much smaller

for an entrance process involving continuous deformation and growth of an initially small vortex segment. Presumably, some such process occurs in real vortex systems or else vortices would not be produced as easily as they are. It would seem that some barrier remains for real systems, because hysteresis in the number of vortices vs. rotation speed has been observed in experiments.[23] In this section we discuss observations which may be relevant to the question of the processes involved in the entrance of vortices.

One might expect the state of the superfluid to depend upon such details as the rotation history of the fluid, the nature of the vessel walls, and the level of vibration of the apparatus. As part of this investigation of vortex phenomena we have studied the first possibility, rotation history dependence. In particular, we have tried to determine how the angular acceleration of the vessel affects the superfluid state, both in terms of the ultimate number of vortices produced and the rate at which they appear.

The observations can be divided into two classes, records of slow ($\sim 10^{-5}$ rad/sec^2) and rapid ($\sim 10^{-2}$ rad/sec^2) acceleration. In all cases constant accelerations were achieved using a digitally derived voltage ramp applied to the drive motor of the apparatus.

A total of eight slow acceleration trials were recorded, Prior to each trial, the apparatus was at rest for at least 1 h. While it would have been interesting to have warmed above the lambda point and recooled before each trial, this procedure was too time-consuming to be implemented.

Figure 15 shows the results of the slow acceleration trials. The lower curve in each plot is the number of vortices observed as a function of time. These data were determined from the motion picture records of each trial. In most cases the number of vortices observed at a given time could be determined unambiguously, but there is an uncertainty of ± 1 for some of the very short-lived states, particularly for trial F. The upper curve in each plot is the angular velocity of the vessel and the middle, steplike curve is the predicted number of vortices for the equilibrium state. The predicted values were obtained using the free energies calculated by Campbell and Ziff[6] with the core parameter set equal to 1.0 Å. The predictions are only weakly dependent on the value of the core parameter.

The observations support the following general statements: (1) the number of vortices observed during and after slow angular acceleration is significantly less than the equilibrium number, (2) transitions involving the appearance of more than one vortex are less likely than single-vortex transitions, (3) the number of vortices observed at a given rotation speed does not depend strongly on the angular acceleration, but the time rate of appearance of vortices is affected, being virtually zero when the rotation speed is held constant. The almost complete lack of transitions during the periods of constant angular velocity indicates that vibrations of the

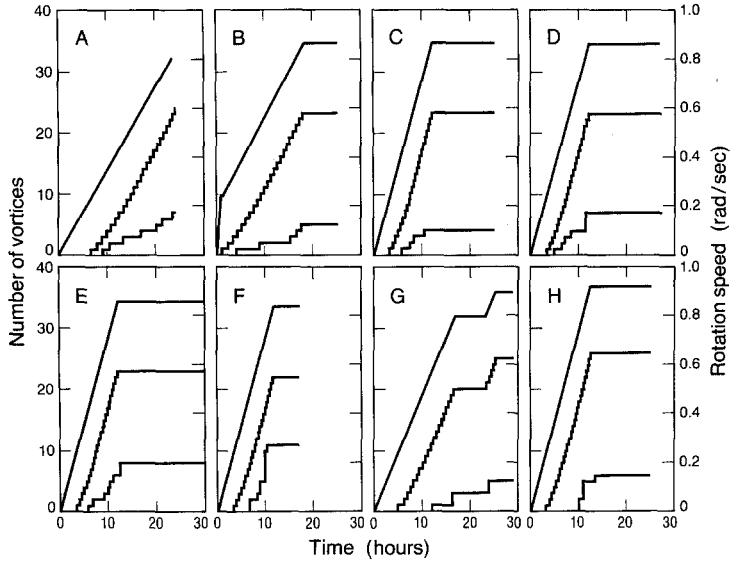

Fig. 15. The results of eight slow acceleration trials. For each trial the upper curve gives the rotation speed (right scale), the middle curve gives the predicted equilibrium number of vortices (left scale), and the lower curve gives the observed vortex number (left scale). All are plotted vs. time.

apparatus are not strong enough to cause transitions in vortex number. We know of no theoretical model which can account for these observations.

The periods of acceleration in the rapid acceleration trials are very short (less than 1 min) and the first vortices do not appear until after the final rotation speed has been reached. Thus, the emphasis in this part of the study is on the response of the superfluid during the constant-rotation-speed periods following rapid accelerations rather than the periods of acceleration themselves. The quantity upon which we have focused is the amount of time between the end of an acceleration period and the appearance of the first vortices. We call this the delay time.

Sequences of trials at a given angular acceleration (typically 0.02 rad/sec^2) and final rotation speed (in the range 0.338–0.750 rad/sec) were obtained by automating the apparatus so that rotation was started and stopped at regular intervals (usually 1 h of rotation and 1 h at rest). Although film records were made during many of the trials, the delay times were determined from strip chart records of the magnitude of the light signal from the vortices. The light was detected by a photomultiplier, which sensed a small fraction of the defocused light output of the image intensifier. Simultaneous film records were made by focusing the remaining light onto the image tube of the television camera. The photomultiplier output was

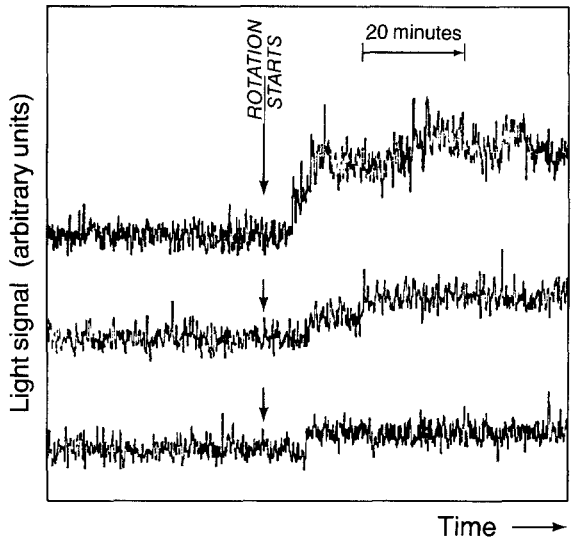

Fig. 16. Plots of the magnitude of the vortex light signal vs. time for three different spinup trials. For each trial the apparatus is accelerated from rest to a fixed rotation speed (0.47 rad/sec for A, 0.34 rad/sec for B and C) at an angular acceleration of 0.02 rad/sec^2. Note that the increase in the light signal (which coincides with the appearance of vortices in the films) occurs several minutes after the start of rotation.

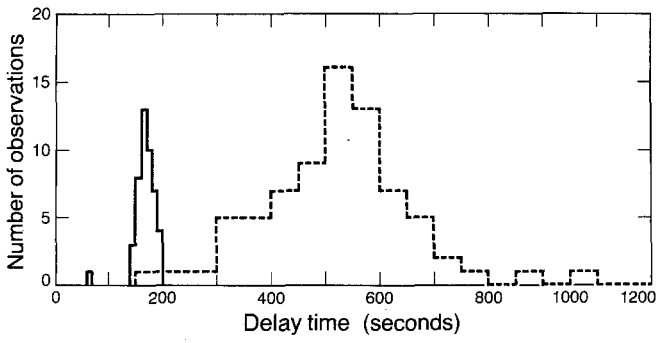

Fig. 17. Histograms showing the distributions of the measured values of the delay time for a large number of repeated spinup trials. The solid curve is for trials having a final rotation speed of 0.600 rad/sec and the dashed curve is for those with a speed of 0.338 rad/sec. The strong dependence of both the mean and standard deviations of these distributions upon final rotation speed can be seen.

electronically integrated for a time equal to the light pulse duration (50 msec). The integrated signal (updated after each charge dump) was recorded on the strip chart. Figure 16 shows several of these light signal records. The steplike increases in the light signal coincide with the appearance of vortices in the film records.

Plotted in Fig. 17 are histograms showing the distributions of measured delay times for two sequences of trials, one for a final rotation speed of 0.338 rad/sec and the other for 0.600 rad/sec. The angular acceleration was 0.020 rad/sec^2 for both sets of trials. The distributions are peaked and can be characterized by a mean value and a width. It can be seen that both of these quantities depend upon rotation speed, becoming smaller with increasing rotation speed.

The rotation speed dependence of the mean delay time is shown more clearly in Fig. 18, which is a plot of the inverse of the mean delay time vs. final rotation speed for data obtained at a variety of rotation speeds. The angular acceleration was 0.02 rad/sec^2 for all of these trials. Most sequences of trials consisted of alternating periods of rest and rotation, each 1 h long, but some of the sequences at higher final rotation speeds were repeated with periods as short as 15 min. The duration of the waiting period before spinup had no noticeable effect on the delay time, provided, of course, that the vortices from the previous spinup were allowed to disappear (always the case for the data presented). The error bars in the figure are the standard deviations of the inverse mean delay times and depend upon the distribution widths and the number of trials in each sequence (the number varies from 15 to 75). The scatter in the data is quite large, but the general trend indicates a possible linear dependence of the inverse delay time on final rotation speed.

The predicted critical rotation speed Ω_{c1} below which a single vortex state has higher free energy than the zero state is indicated in Fig. 18. Extrapolation of the delay time data indicates that the speed at which the delay time would diverge is near this critical speed. This might mean that the free energy difference between the state with zero vortices and the state with one vortex (a difference which is proportional to $\Omega - \Omega_{c1}$) plays an important role in the processes responsible for the appearance of vortices, even when more than one line appears. Because of the divergence of the delay time, measurements of the delay time distributions become increasingly time-consuming as the rotation speed is lowered. For this reason, the observations were not extended to speeds lower than that shown in the figure.

Because the widths of the measured delay time distributions generally exceed the instrumental time resolution (the charging cycle time is 10 sec), they presumably reflect, in some way, the underlying processes responsible

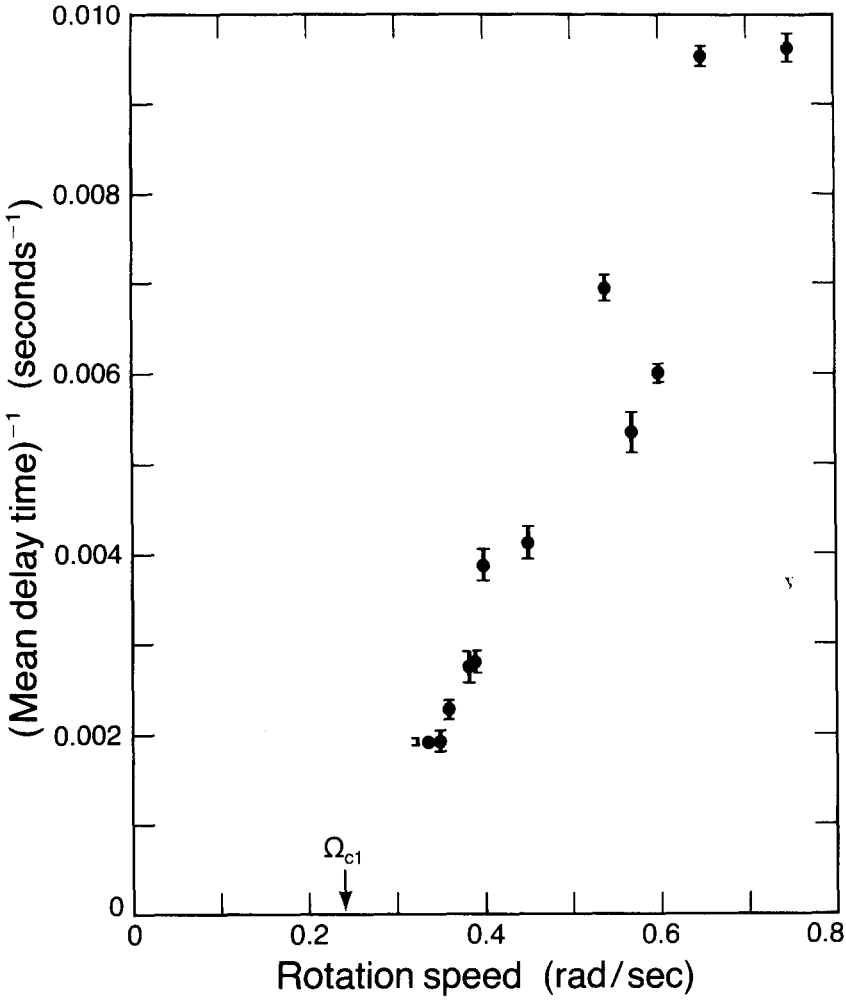

Fig. 18. A plot of the inverse of the mean delay time vs. final rotation speed. The value of the predicted critical rotation speed Ω_{c1} at which the first vortex would enter (in the absence of free energy barriers) is indicated on the horizontal axis.

for spinup phenomena. The dependence of the distribution widths on rotation speed is similar to that of the mean delay time. This point is most clearly illustrated by plotting the standard deviations of the distributions versus their mean delay time, as in Fig. 19.

The results discussed so far are for an angular acceleration of 0.020 rad/sec^2. Data from sequences of trials at several different angular accelerations but with a fixed final rotation speed were also obtained. The

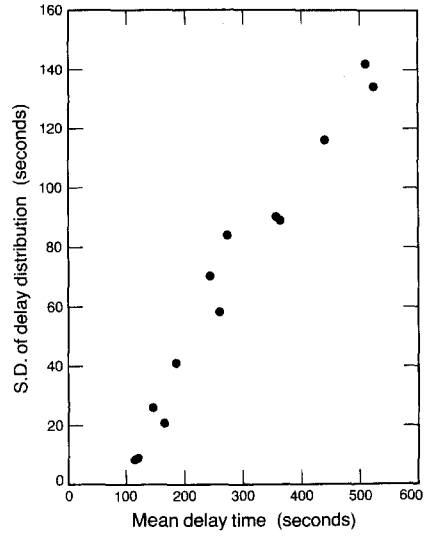

Fig. 19. A plot of the standard deviation of the measured delay time distributions vs. the mean delay time.

results (for two different final rotation speeds) are shown in Fig. 20 as plots of the mean delay time vs. angular acceleration. Also shown are the amounts of time required for the period of acceleration. As we have defined it, the delay time is the time between the end of the acceleration period and the appearance of the first vortices. It can be seen that, defined in this way, the mean delay time shows no significant dependence upon angular acceleration. Had the acceleration time been included in the delay time, this would not be true.

At very low accelerations, like those of the slow acceleration study, the concept of a delay time breaks down. In such cases the vortices often

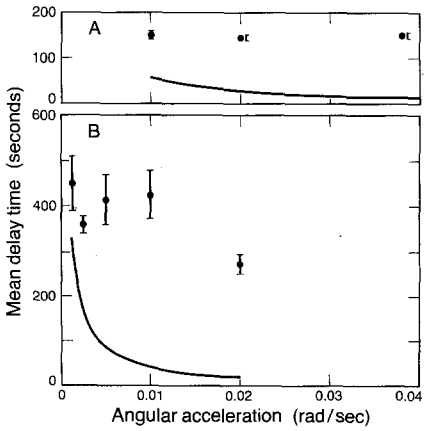

Fig. 20. Plots of the mean delay time vs. angular acceleration for two different final rotation speeds: (A) 0.54 rad/sec, (B) 0.42 rad/sec. The solid curves show the amount of time spent during the acceleration period (i.e., the final rotation speed divided by the angular acceleration). This acceleration time is not included in the measured delay times because the delays were measured from the end of the acceleration period to the time of the first vortex appearance.

appear during the acceleration period itself and almost never during the constant-rotation-speed periods. At the lowest acceleration studied (the point at 1.25×10^{-3} rad/sec in Fig. 20B) unusual effects were observed. In three out of the twelve sequential trials (the fifth, sixth, and eleventh) no vortices appeared during the entire hour of rotation. (These trials were excluded from the average for the mean delay time.) Delay times of 1 h (or more) lie well outside the distribution of delay times for the remaining trials and did not occur for any of the trials at higher accelerations. This behavior may signify the qualitative changes which occur in making the transition between the very different regimes of rapid and slow accelerations.

Vortices that do not intersect the free surface of the liquid or are too short to collect sufficient charge are not detected in this experiment. Thus, many possibilities can be imagined for the conditions and processes that take place during and after acceleration of the vessel, all of which can remain hidden from view. The surprising feature of the observations is that simple trends are present. While spinup phenomena are undoubtedly complex in their details, the observation of regularities in behavior suggests that an understanding of at least the dominant underlying processes may be possible.

5. SUMMARY

In summary, we have obtained motion picture records of the positions of quantized vortex lines at the free surface of superfluid ^{4}He. The records correspond to approximately 1000 h of filming under a variety of rotation conditions. The vortices form arrays which are stationary in the rotating frame of reference. In both size and shape, the observed stationary arrays are in reasonable agreement with the predictions of rectilinear vortex theory for singly quantized lines. The random motion of the vortices is measured to be as small as 15 μm and is only slightly greater than the diameter of an individual fiber in the image conduit.

Instances have been found in which arrays of small numbers of lines undergo low-frequency azimuthal oscillations. These appear to be understandable within the framework of ideal vortex theory provided vortex flexure is taken into account. A distinctive type of oscillatory motion (one involving distortion rather than rotation) has been observed for an array of three vortices. The observed motion is similar to that of a predicted normal mode for a three-line array.

Making use of both the film records and measurements of the vortex light signal, we find surprising regularities in the rate of appearance of vortices during and following angular accelerations of the vessel. During

slow accelerations of the vessel, vortices appear at a roughly uniform rate, but there are always fewer vortices than expected for the true equilibrium state. Following a slow acceleration, the apparent vortex number remains essentially constant. For rapid accelerations the converse is observed; vortices only appear after the acceleration has ceased. The amount of time between the end of the acceleration period and the appearance of the first vortices seems to be a well-defined quantity which depends strongly upon the final rotation speed of the vessel.

ACKNOWLEDGMENTS

We wish to thank L. J. Campbell for his helpful comments regarding many aspects of this work. We are also grateful to J. P. Eisenstein, S. Garrett, and G. Swift for valuable discussions and to G. A. Williams and M. J. V. Gordon for their contributions to the development of the apparatus. The low-light-level television camera was generously loaned to us by the Lawrence Livermore Laboratory. The use of a film scanning machine was made possible through the efforts of D. Chapman.

REFERENCES

1. G. A. Williams and R. E. Packard, *J. Low Temp. Phys.* **39**, 553 (1980).
2. E. J. Yarmchuk, M. J. V. Gordon, and R. E. Packard, *Phys. Rev. Lett.* **43**, 214 (1979).
3. T. C. Fry, *Am. Math. Monthly* **39**, 199 (1932).
4. G. B. Hess, *Phys. Rev.* **161**, 189 (1967).
5. D. Stauffer and A. L. Fetter, *Phys. Rev.* **168**, 156 (1968).
6. L. J. Campbell and R. M. Ziff, *Phys. Rev. B* **20**, 1886 (1979).
7. L. J. Campbell and R. M. Ziff, Los Alamos Scientific Laboratory Report No. LA-7384-MS (1978), unpublished.
8. G. A. Williams and R. E. Packard, *Phys. Rev. Lett.* **33**, 280 (1974).
9. H. Lamb, *Hydrodynamics* (Dover, New York, 1945), Sect. 157.
10. Lord Kelvin, *Mathematical and Physical Papers* (1878), Vol. IV, p. 135.
11. T. H. Havelock, *Phil. Mag.* **11**, 617 (1931).
12. D. Stauffer and A. L. Fetter, *Phys. Rev.* **168**, 156 (1968).
13. M. R. Williams and A. L. Fetter, *Phys. Rev. B* **16**, 4846 (1977).
14. W. Thomson, *Phil. Mag.* **10**, 155 (1980).
15. E. S. Raja Gopal, *Ann. Phys. (N.Y.)* **29**, 350 (1964).
16. H. E. Hall, *Proc. Roy. Soc. (London)* A **245**, 546 (1958); S. D. Tsakadze, *Fiz. Nizk. Temp.* **4**, 148 (1978) [*Sov. J. Low Temp. Phys.* **4**, 72 (1978)].
17. C. D. Andereck, J. Chalupa, and W. I. Glaberson, *Phys. Rev. Lett.* **44**, 33 (1980).
18. R. A. Ashton and W. I. Glaberson, *Phys. Rev. Lett.* **42**, 1062 (1979).
19. E. B. Sonin, *Zh. Eksp. Teor. Fiz.* **70**, (1976) [*Sov. Phys.—JETP* **43**, 1027 (1976).
20. G. W. Rayfield and F. Reif, *Phys. Rev.* **136**, A1194 (1964).
21. H. E. Hall and W. F. Vinen, *Proc. Roy. Soc. (London)* A **238**, 215 (1956).
22. G. A. Williams and R. E. Packard, *J. Low Temp. Phys.* **33**, 459 (1978); R. M. Ostermeier and W. I. Glaberson, *J. Low Temp Phys.* **25**, 317 (1976).
23. R. E. Packard and T. M. Sanders, *Phys. Rev. Lett.* **22**, 823 (1969).